

Accelerating cosmologies tested by distance measures

V. Barger¹, Y. Gao¹ and D. Marfatia²

¹*Department of Physics, University of Wisconsin, Madison, WI 53706*

²*Department of Physics and Astronomy, University of Kansas, Lawrence, KS 66045*

Abstract

We test if the latest Gold set of 182 SNIa or the combined “Platinum” set of 192 SNIa from the ESSENCE and Gold sets, in conjunction with the CMB shift parameter show a preference between the Λ CDM model, three w CDM models, and the DGP model of modified gravity as an explanation for the current accelerating phase of the universe’s expansion. We consider flat w CDM models with an equation of state $w(a)$ that is (i) constant with scale factor a , (ii) varies as $w_0 + w_a(1 - a)$ for redshifts probed by supernovae but is fixed at -1 at earlier epochs and (iii) varies as $w_0 + w_a(1 - a)$ since recombination. We find that all five models explain the data with comparable success.

Observations of Type Ia supernovae (SNIa), the cosmic microwave background, and large scale structure corroborate that the expansion of our universe is accelerating. Explanations of this acceleration often invoke the existence of a dark energy component with the unusual property of negative pressure [1]. The simplest example of dark energy is the cosmological constant Λ with an equation of state $w \equiv p/\rho = -1$. Although in the context of Λ , p and ρ are the effective pressure and energy density attributed to vacuum energy, in general they are the corresponding quantities of the fluid describing dark energy. Possibilities with a time-varying equation of state are modelled by introducing a scalar field called quintessence [2]. No dark energy model has a natural explanation. Explanations of the current acceleration that avoid the introduction of dark energy emerge from modifications to gravity, typically in the context of braneworld models.

For models with dark energy, we consider the nonflat Λ CDM model, and three flat universe models with equations of state that differ from -1 at some time in the expansion history. We refer to these as flat w CDM models. The simplest of these has a constant w that differs from -1 . To model dark energy with a time-varying w , we adopt a parameterization that is well-behaved at high redshift: $w(a) = w_0 + w_a(1 - a)$ [3], where a is normalized such that it is equal to 1 today and is related to redshift z by $a = 1/(1 + z)$. While this parameterization reduces to the linear relation $w(z) = w_0 + w_a z$ [4] at low redshifts, it has the disadvantage that when analyzing high-redshift data, we are implicitly restricting ourselves to models that are well-represented by this time evolution. Said differently, we are placing the strict prior that dark energy must have evolved in this manner throughout. Keeping the latter in mind, one case we consider is that dark energy evolves according to $w(a) = w_0 + w_a(1 - a)$ for redshifts probed by SNIa and behaves like a cosmological constant at earlier epochs. A second case, involving a stronger prior, is that $w(a) = w_0 + w_a(1 - a)$ is valid till the epoch of last scattering.

The Friedman equation in dimensionless form with $H \equiv \dot{a}/a$ and $H_0 \equiv H(z = 0)$ is

$$\frac{H(z)^2}{H_0^2} = \Omega_m(1+z)^3 + \Omega_w(1+z)^{3(1+w_0+w_a)} e^{-3w_a \frac{z}{1+z}} + \Omega_k(1+z)^2, \quad (1)$$

where Ω_m , Ω_w and Ω_k are the matter, dark energy and curvature densities in units of the critical density. For the Λ CDM model, $\Omega_w \equiv \Omega_\Lambda$, $w_0 = -1$ and $w_a = 0$. For flat models, $\Omega_k = 1 - \Omega_m - \Omega_w = 0$.

The DGP model [5] (named so for its authors) is a generally-covariant infrared modification of general relativity (GR) and is not reducible to an extension of GR with additional scalar or vector degrees of freedom. At short distances gravity is 4-dimensional, while in the far infrared, gravity appears to be 5-dimensional because of gravitational leakage from the 4-dimensional brane into the 5-dimensional bulk. The implications for cosmology are that at early times the correction from the infrared modification is negligible and the universe obeys the standard cosmology. However, at late times, the weakening of gravity is significant and leads to self-accelerated expansion without the need for any form of matter [6]. Due its firm theoretical foundation [7], we analyze the DGP model

as the canonical example of modified GR that explains the current acceleration without the need for dark energy.

The Hubble expansion is given by [6]

$$\frac{H(z)^2}{H_0^2} = [\sqrt{\Omega_r} + \sqrt{\Omega_r + \Omega_m(1+z)^3}]^2 + \Omega_k(1+z)^2. \quad (2)$$

Here $\Omega_r \equiv (4r_c^2 H_0^2)^{-1}$, where $r_c \equiv M_4^2/(2M_5^3)$ is the length scale beyond which 4-dimensional gravity (with Planck scale M_4) transits to 5-dimensional gravity (with Planck scale M_5). Setting $z = 0$ in Eq. (2) yields $\Omega_k = 1 - [\sqrt{\Omega_r} + \sqrt{\Omega_r + \Omega_m}]^2$. Note that the DGP model has the same number of parameters as Λ CDM, with Ω_r replacing Ω_Λ .

To compare the various models on an equal-footing, we only analyze data that probe the expansion history of the universe. We do not utilize data that are sensitive to the evolution of density perturbations since these have not been fully worked out for the DGP model, although progress has been made in Ref. [8]. We analyze the distance moduli of the Gold set of 182 SN [9] (of which 16 have $z > 1$) compiled from Refs. [10, 11, 12] and the ‘‘Platinum’’ set of 192 SN [13] compiled from the ESSENCE [14] and Gold sets. In our analyses, we include the CMB shift parameter [15] which measures the distance to the last scattering surface. For most of what follows, we do not use the baryon acoustic oscillation (BAO) distance parameter A extracted from the scale corresponding to the first acoustic peak at recombination [16]. The procedure used to determine A assumes that w does not vary with redshift. The resulting value may not be applicable for time-varying w [17], making it unsuitable for three of the five models we are considering. Recent joint analyses of the DGP model with older data in various combinations (with some including the A parameter) can be found in Ref. [18].

The shift parameter, defined in terms of the H_0 -independent luminosity distance $D_L = H_0 d_L$ (where d_L is the luminosity distance) [15]:

$$R \equiv \sqrt{\Omega_m} \frac{D_L(z_{CMB})}{(1+z_{CMB})}, \quad (3)$$

is approximately equivalent to the ratio of the sound horizon at recombination to the comoving distance to the last scattering surface. For all practical purposes, R is model-independent. We use the value $R = 1.70 \pm 0.03$ [19] obtained from the WMAP 3-year data [20] with a redshift at recombination $z_{CMB} = 1089 \pm 1$.

The statistical significance of a model is determined by evaluating $\chi_R^2 = (R^{obs} - R^{th})^2/\sigma_R^2$ and χ_{SN}^2 , which after marginalization over a nuisance parameter, has the absolute value [21]

$$\chi_{SN}^2 = A - \frac{B^2}{C}, \quad (4)$$

where

$$A = \sum_{i=1}^N \frac{(\mu_i^{obs} - 5 \log_{10} D_L(z_i))^2}{\sigma_i^2}, \quad B = \sum_{i=1}^N \frac{\mu_i^{obs} - 5 \log_{10} D_L(z_i)}{\sigma_i^2}, \quad C = \sum_{i=1}^N \frac{1}{\sigma_i^2}.$$

Here, μ_i^{obs} and σ_i are the distance modulus and its uncertainty at redshift z_i . $N = 182$ for the Gold set and $N = 192$ for the Platinum set.

Λ CDM: In Fig. 1 we display the results of our analysis of the nonflat Λ CDM model. The shaded regions are the 1σ , 2σ and 3σ allowed regions from an analysis of the latest SN data (upper panel: Gold set, lower panel: Platinum set) and of the CMB shift parameter R . Although expected, the orthogonality of the regions is striking. The solid contours depict the corresponding regions from the joint analysis. The best-fit parameters are provided in Table 1. The dot marks the best-fit from the joint analysis. Notice that the combined analyses prefer universes that are almost flat with a tendency for positive curvature. If we restrict ourselves to flat universes, the minimum χ^2 value for the joint analysis with the Gold set (Platinum set) increases to 163 (196.3), and the best-fit moves to $\Omega_m = 0.3$ ($\Omega_m = 0.25$); χ_{SN}^2 increases to 158.6 for the Gold set but remains essentially unchanged for the Platinum set.

Flat w CDM with constant w : We allow w to take values different from -1 , but do not allow for time variation by setting $w_a = 0$. Figure 2 is similar to Fig. 1 except that we plot w_0 vs Ω_m . Keeping in mind that the number of degrees of freedom is the same as that for the Λ CDM model, we see that the fit to the Λ CDM model is not significantly better; with the Gold set (Platinum set) it has a minimum χ^2 that is only 1.8 (0.3) lower.

Flat w CDM with late-varying w : In this case, w has time-variation only from $z = 1.8$ until today, and equals -1 at earlier times. We also require $0.15 \leq \Omega_m \leq 0.35$. In Fig. 3, we only show the 1σ and 2σ regions for the separate SN and R analyses for obvious reasons. It is no surprise that the R parameter shows no sensitivity to w_a because we have assumed that the dark energy behaves as a cosmological constant since recombination until $z = 1.8$. This assumption eliminates the constraining power of R that comes from its long lever arm. The joint constraint is dominated by the SN data. This is evident from Fig. 3 and Table 1. The allowed regions and best-fit point do not move significantly on adding the R parameter to the analysis. Although the Gold and Platinum sets favor different regions of w_a , on comparing the allowed regions with the regions occupied by different dark energy models in the (w_0, w_a) plane, as classified in Ref. [22], it is clear that no class of models is excluded even at the 2σ C. L. by either dataset.

Flat w CDM with varying w : The equation of state is allowed to vary since recombination. Again, we require $0.15 \leq \Omega_m \leq 0.35$. As expected, the results of analyzing SN data alone are identical with that of late-varying w since there are no SN data with $z > 1.8$. See Table 1 and

	Gold (182 SN)			Platinum (192 SN)		
Λ CDM	χ^2	Ω_Λ	Ω_m	χ^2	Ω_Λ	Ω_m
SN	156.4	0.95	0.48	195.2	0.85	0.33
SN+ R	158.4	0.68	0.36	195.6	0.74	0.27
SN+ R +BAO	161.4	0.72	0.30	195.6	0.74	0.27
w CDM, $w_a = 0$	χ^2	w_0	Ω_m	χ^2	w_0	Ω_m
SN	156.6	-1.75	0.46	195.4	-1.16	0.31
SN+ R	160.2	-0.85	0.28	195.9	-0.94	0.24
SN+ R +BAO	160.3	-0.86	0.29	196.6	-0.98	0.26
w CDM, $w(z > 1.8) = -1$	χ^2	w_0	w_a	χ^2	w_0	w_a
SN	156.5	-1.11	2.39	195.3	-1.11	-1.16
SN+ R	156.5	-1.28	2.69	195.5	-1.06	0.81
w CDM	χ^2	w_0	w_a	χ^2	w_0	w_a
SN	156.5	-1.11	2.39	195.3	-1.11	-1.16
SN+ R	157.0	-1.35	1.54	195.5	-1.09	0.67
DGP	χ^2	Ω_r	Ω_m	χ^2	Ω_r	Ω_m
SN	156.4	0.24	0.36	195.1	0.22	0.24
SN+ R	160.3	0.14	0.23	196.4	0.16	0.17

Table 1: The minimum χ^2 values and best-fit parameters for each of the five models. The χ^2 per degree of freedom is substantially different for the Gold and Platinum datasets. All w CDM models are flat. In the analyses in which both w_0 and w_a are allowed to vary freely, we require that Ω_m take values between 0.15 and 0.35. All five models have $\chi_R^2 = 0$ at the minimum in the analysis of the shift parameter alone. We do not show the corresponding best-fit parameters because the χ_R^2 distributions are too broad for the parameters to be meaningful. We have included the BAO constraint for the two models with a constant w for comparison. The number of parameters in the analyses of the successive models are 3, 3, 4, 4, 3, respectively, where in each case one parameter is a nuisance parameter that is marginalized over.

Figs. 3 and 4. From Fig. 4, we now see how R helps to constrain w_a . Nevertheless, all the dark energy models classified in Ref. [22] remain safe. With respect to Λ CDM, the additional free parameter improves the minimum χ^2 of the joint analysis with the Gold set (Platinum set) by only 1.4 (0.1).

DGP: Figure 5 is similar to Fig. 1 with Ω_Λ replaced by the physical parameter relevant to DGP, Ω_r . A similar orthogonal relationship exists between the SN and R regions. However, here

we see that the joint analysis with the Gold set (Platinum set) prefers a slightly open universe with $\Omega_k = 0.027 \pm 0.014$ ($\Omega_k = 0.041 \pm 0.010$). The overall fit is only slightly worse compared to Λ CDM.

To assess the impact of the BAO constraint on the two models that do not have a time-varying equation of state (Λ CDM and the w CDM model with constant w), we use the measured value $A = 0.469 \pm 0.017$ [16], where

$$A \equiv \sqrt{\Omega_m} \left[\frac{H_0}{H(z_{BAO})} \left(\frac{D_L(z_{BAO})}{z_{BAO}(1+z_{BAO})} \right)^2 \right]^{1/3}, \quad (5)$$

to calculate $\chi_A^2 = (A^{obs} - A^{th})^2 / \sigma_A^2$. Here, $z_{BAO} = 0.35$ is the typical redshift of the SDSS sample of luminous red galaxies. From Figs. 6 and 7, it can be seen that the BAO constraint provides a satisfying confirmation that the different datasets are concordant, and helps to further constrain the regions from the joint analysis of SN data and R . The minimum χ^2 and best-fit parameters from the joint analyses including the BAO constraint are provided in Table 1. For the Λ CDM model, the addition of this datapoint to the joint analysis with the Gold set results in a preference for a universe with less curvature at the expense of increasing the minimum χ^2 by 3. The BAO constraint has no effect on the best-fit parameters of the Λ CDM model in a joint analysis with the Platinum set.

In conclusion, it is noteworthy that all 5 models fit the SN data equally well. Only on inclusion of R in the analyses do minor differences develop. Current data cannot tell if the accelerated expansion is caused by a cosmological constant, by dark energy with a constant w , by dark energy whose equation of state started varying recently or has always been varying, or due to modified gravitational physics of conventional matter¹. A detailed understanding of how density perturbations evolve in braneworld cosmologies will enable the use of the vast amount of data available on the power spectrum from observations of the CMB and large scale structure and may help with the basic question of whether the acceleration is due to a new form of energy or due to new aspects of gravity. A step forward from kinematical probes of modified gravity to dynamical ones is the order of the day.

Acknowledgments. We thank Ned Wright for a communication. This research was supported by the U.S. Department of Energy under Grants No. DE-FG02-95ER40896 and DE-FG02-04ER41308 and by the NSF under CAREER Grant No. PHY-0544278. Computations were performed on facilities supported by the NSF under Grants No. EIA-032078 (GLOW), PHY-0516857 (CMS Research Program subcontract from UCLA), and PHY-0533280 (DISUN), and by the Wisconsin Alumni Research Foundation.

¹Other analyses of similar datasets can be found in Ref. [23].

References

- [1] For a recent review see, E. J. Copeland, M. Sami and S. Tsujikawa, arXiv:hep-th/0603057.
- [2] P. J. E. Peebles and B. Ratra, *Astrophys. J.* **325**, L17 (1988); B. Ratra and P. J. E. Peebles, *Phys. Rev. D* **37**, 3406 (1988); C. Wetterich, *Nucl. Phys. B* **302**, 668 (1988).
- [3] M. Chevallier and D. Polarski, *Int. J. Mod. Phys. D* **10**, 213 (2001) [arXiv:gr-qc/0009008]; E. V. Linder, *Phys. Rev. Lett.* **90**, 091301 (2003) [arXiv:astro-ph/0208512].
- [4] I. Maor, R. Brustein and P. J. Steinhardt, *Phys. Rev. Lett.* **86**, 6 (2001) [Erratum-ibid. **87**, 049901 (2001)] [arXiv:astro-ph/0007297]; J. Weller and A. Albrecht, *Phys. Rev. Lett.* **86**, 1939 (2001) [arXiv:astro-ph/0008314]; V. D. Barger and D. Marfatia, *Phys. Lett. B* **498**, 67 (2001) [arXiv:astro-ph/0009256].
- [5] G. R. Dvali, G. Gabadadze and M. Porrati, *Phys. Lett. B* **485**, 208 (2000) [arXiv:hep-th/0005016].
- [6] C. Deffayet, *Phys. Lett. B* **502**, 199 (2001) [arXiv:hep-th/0010186]; C. Deffayet, G. R. Dvali and G. Gabadadze, *Phys. Rev. D* **65**, 044023 (2002) [arXiv:astro-ph/0105068].
- [7] For a review see, A. Lue, *Phys. Rept.* **423**, 1 (2006) [arXiv:astro-ph/0510068].
- [8] K. Koyama and R. Maartens, *JCAP* **0601**, 016 (2006) [arXiv:astro-ph/0511634]; I. Sawicki, Y. S. Song and W. Hu, arXiv:astro-ph/0606285; Y. S. Song, I. Sawicki and W. Hu, arXiv:astro-ph/0606286.
- [9] The Gold dataset is available at <http://braeburn.pha.jhu.edu/~ariess/R06>
- [10] A. G. Riess *et al.*, arXiv:astro-ph/0611572.
- [11] P. Astier *et al.*, *Astron. Astrophys.* **447**, 31 (2006) [arXiv:astro-ph/0510447].
- [12] A. G. Riess *et al.* [Supernova Search Team Collaboration], *Astrophys. J.* **607**, 665 (2004) [arXiv:astro-ph/0402512].
- [13] T. M. Davis *et al.*, arXiv:astro-ph/0701510. What we have dubbed the “Platinum” dataset is available at <http://dark.dark-cosmology.dk/~tamarad/SN/> or <http://www.ctio.noao.edu/essence/> or <http://braeburn.pha.jhu.edu/~ariess/R06>
- [14] W. M. Wood-Vasey *et al.*, arXiv:astro-ph/0701041.
- [15] J. R. Bond, G. Efstathiou and M. Tegmark, *Mon. Not. Roy. Astron. Soc.* **291**, L33 (1997) [arXiv:astro-ph/9702100].

- [16] D. J. Eisenstein *et al.* [SDSS Collaboration], *Astrophys. J.* **633**, 560 (2005) [arXiv:astro-ph/0501171].
- [17] J. Dick, L. Knox and M. Chu, *JCAP* **0607**, 001 (2006) [arXiv:astro-ph/0603247].
- [18] M. Fairbairn and A. Goobar, *Phys. Lett. B* **642**, 432 (2006) [arXiv:astro-ph/0511029]; R. Maartens and E. Majerotto, *Phys. Rev. D* **74**, 023004 (2006) [arXiv:astro-ph/0603353]; Z. K. Guo, Z. H. Zhu, J. S. Alcaniz and Y. Z. Zhang, *Astrophys. J.* **646**, 1 (2006) [arXiv:astro-ph/0603632]; D. A. Dicus and W. W. Repko, arXiv:astro-ph/0610232.
- [19] Y. Wang and P. Mukherjee, arXiv:astro-ph/0604051.
- [20] D. N. Spergel *et al.*, arXiv:astro-ph/0603449.
- [21] E. Di Pietro and J. F. Claeskens, *Mon. Not. Roy. Astron. Soc.* **341**, 1299 (2003) [arXiv:astro-ph/0207332]; L. Perivolaropoulos, *Phys. Rev. D* **71**, 063503 (2005) [arXiv:astro-ph/0412308].
- [22] V. Barger, E. Guarnaccia and D. Marfatia, *Phys. Lett. B* **635**, 61 (2006) [arXiv:hep-ph/0512320].
- [23] H. Li, M. Su, Z. Fan, Z. Dai and X. Zhang, arXiv:astro-ph/0612060; Y. G. Gong and A. z. Wang, arXiv:astro-ph/0612196; U. Alam, V. Sahni and A. A. Starobinsky, arXiv:astro-ph/0612381; K. Dutta and L. Sorbo, arXiv:astro-ph/0612457; J. F. Zhang, X. Zhang and H. Y. Liu, arXiv:astro-ph/0612642; S. Nesseris and L. Perivolaropoulos, arXiv:astro-ph/0612653; G. B. Zhao, J. Q. Xia, H. Li, C. Tao, J. M. Virey, Z. H. Zhu and X. Zhang, arXiv:astro-ph/0612728; K. Ichikawa and T. Takahashi, arXiv:astro-ph/0612739; H. Wei, N. N. Tang and S. N. Zhang, arXiv:astro-ph/0612746; P. Serra, A. Heavens and A. Melchiorri, arXiv:astro-ph/0701338; M. S. Movahed, M. Farhang and S. Rahvar, arXiv:astro-ph/0701339; X. Zhang and F. Q. Wu, arXiv:astro-ph/0701405; L. I. Xu, C. W. Zhang, B. R. Chang and H. Y. Liu, arXiv:astro-ph/0701490. S. Rydbeck, M. Fairbairn and A. Goobar, arXiv:astro-ph/0701495; L. I. Xu, C. W. Zhang, B. R. Chang and H. Y. Liu, arXiv:astro-ph/0701519; E. L. Wright, arXiv:astro-ph/0701584.

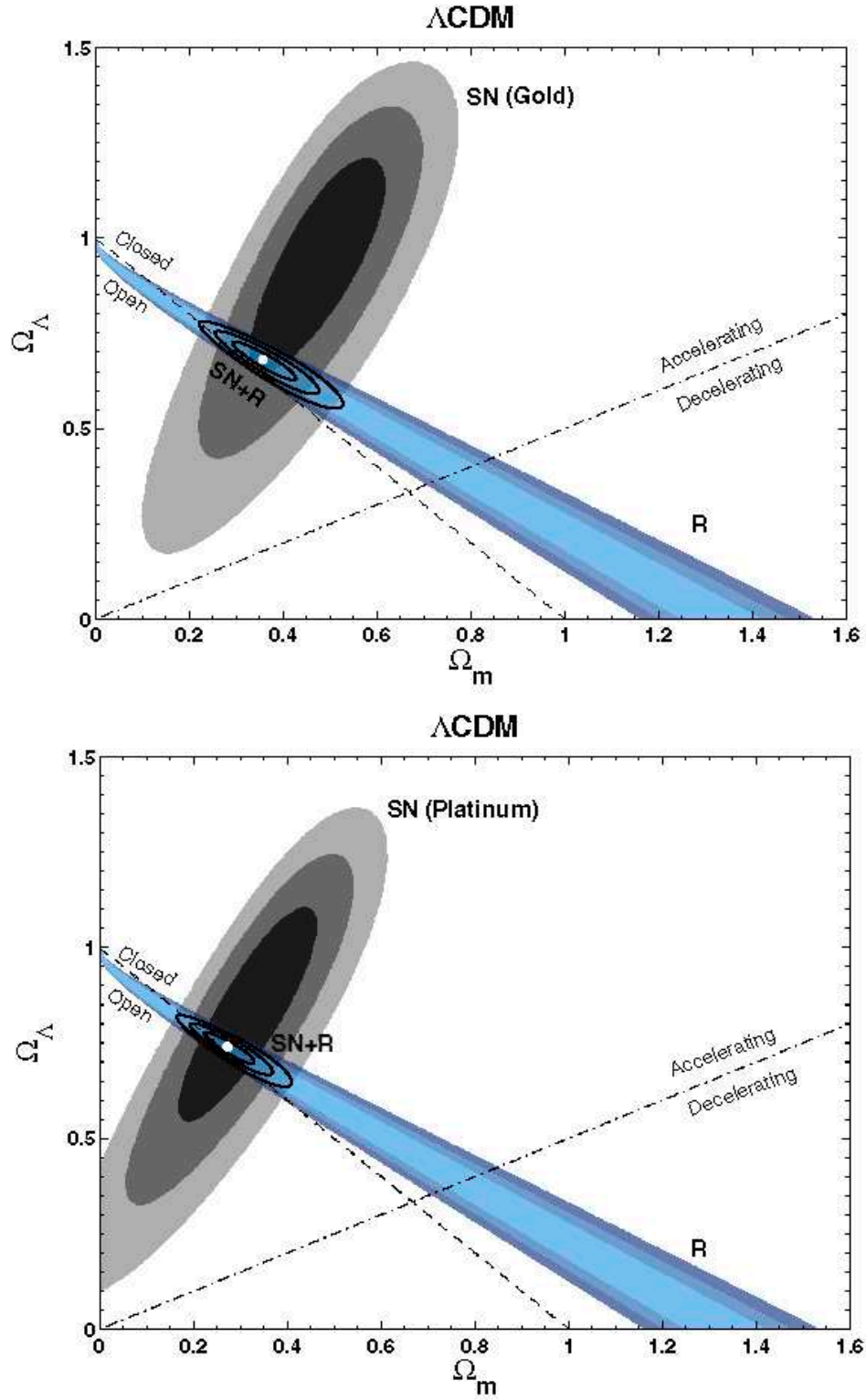


Figure 1: The 1σ , 2σ and 3σ allowed regions for the Λ CDM model from an analysis of SN data (upper panel: Gold set, lower panel: Platinum set) of the CMB shift parameter R and from a joint analysis. The best-fit parameters from the joint analyses are indicated by a dot. See Table 1.

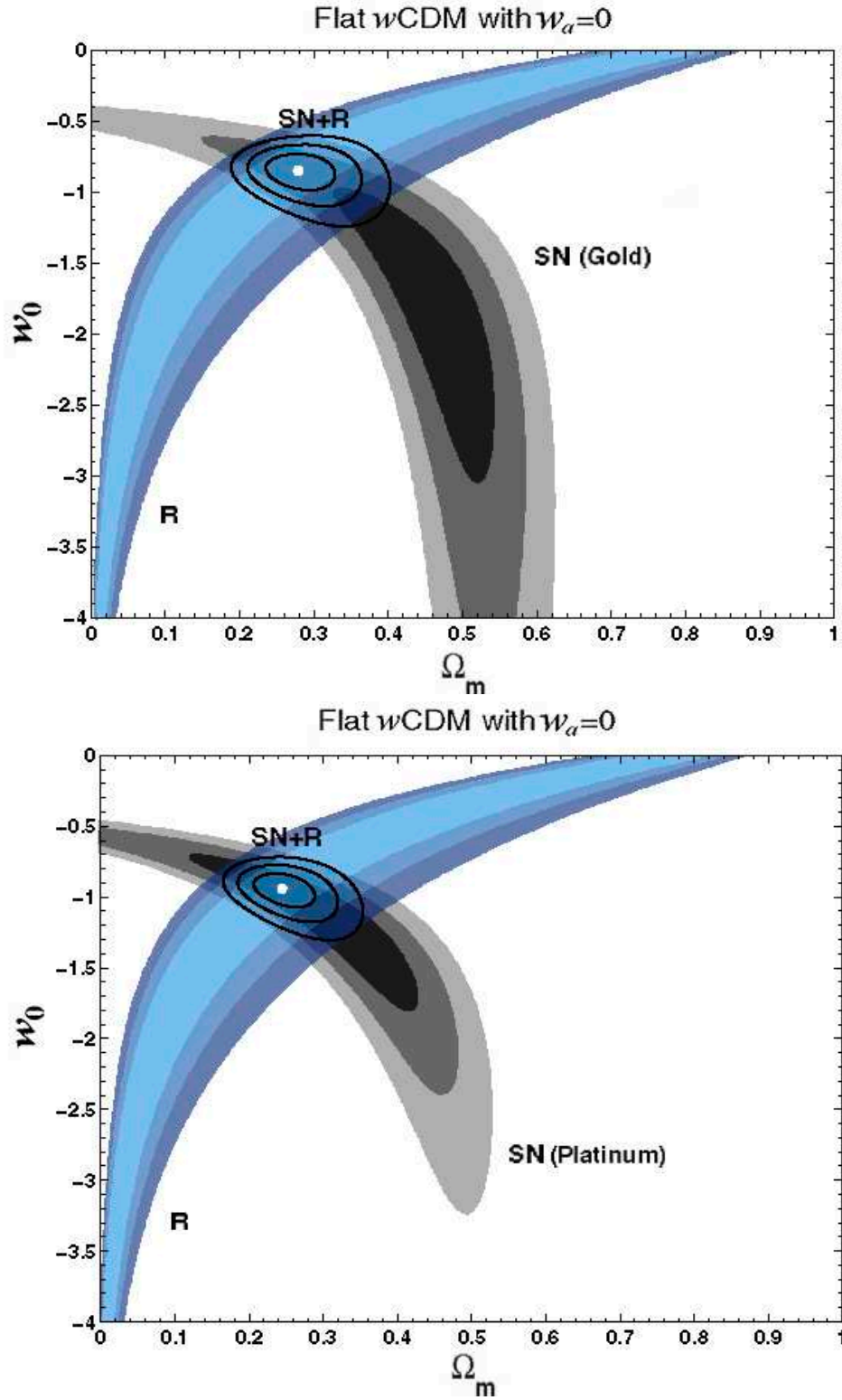


Figure 2: Similar to Fig. 1, but for the w CDM model with a constant equation of state $w(a) = w_0$.

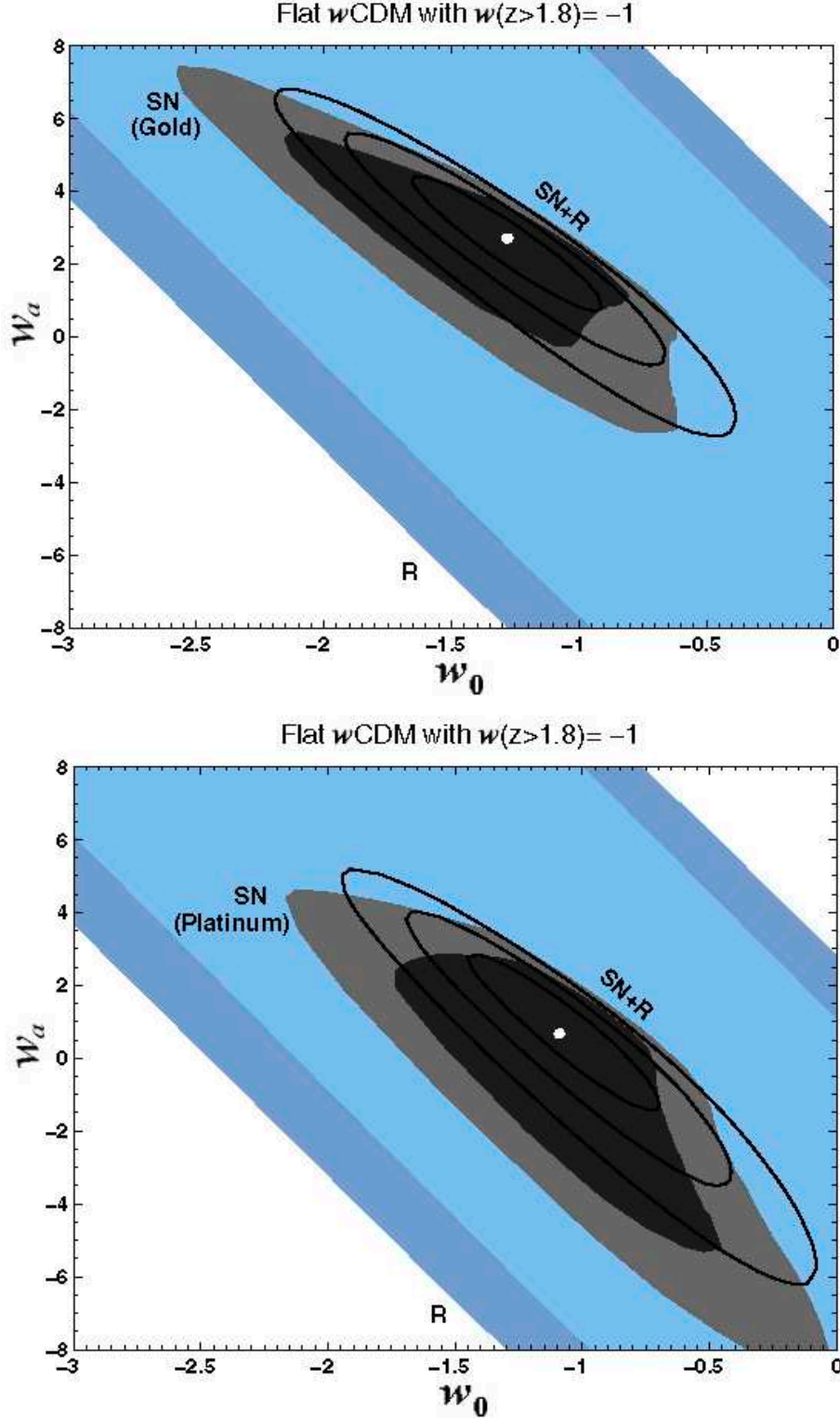


Figure 3: The allowed regions for the flat w CDM model with an equation of state $w(a) = w_0 + w_a(1 - a)$ in the redshift range $0 \leq z \leq 1.8$ and a constant equation of state $w = -1$ for $z > 1.8$. Only the 1σ and 2σ regions are shown for separate SN and R analyses, while the 3σ region is also shown for the joint analysis. The best-fit parameters from the joint analysis are indicated by a dot.

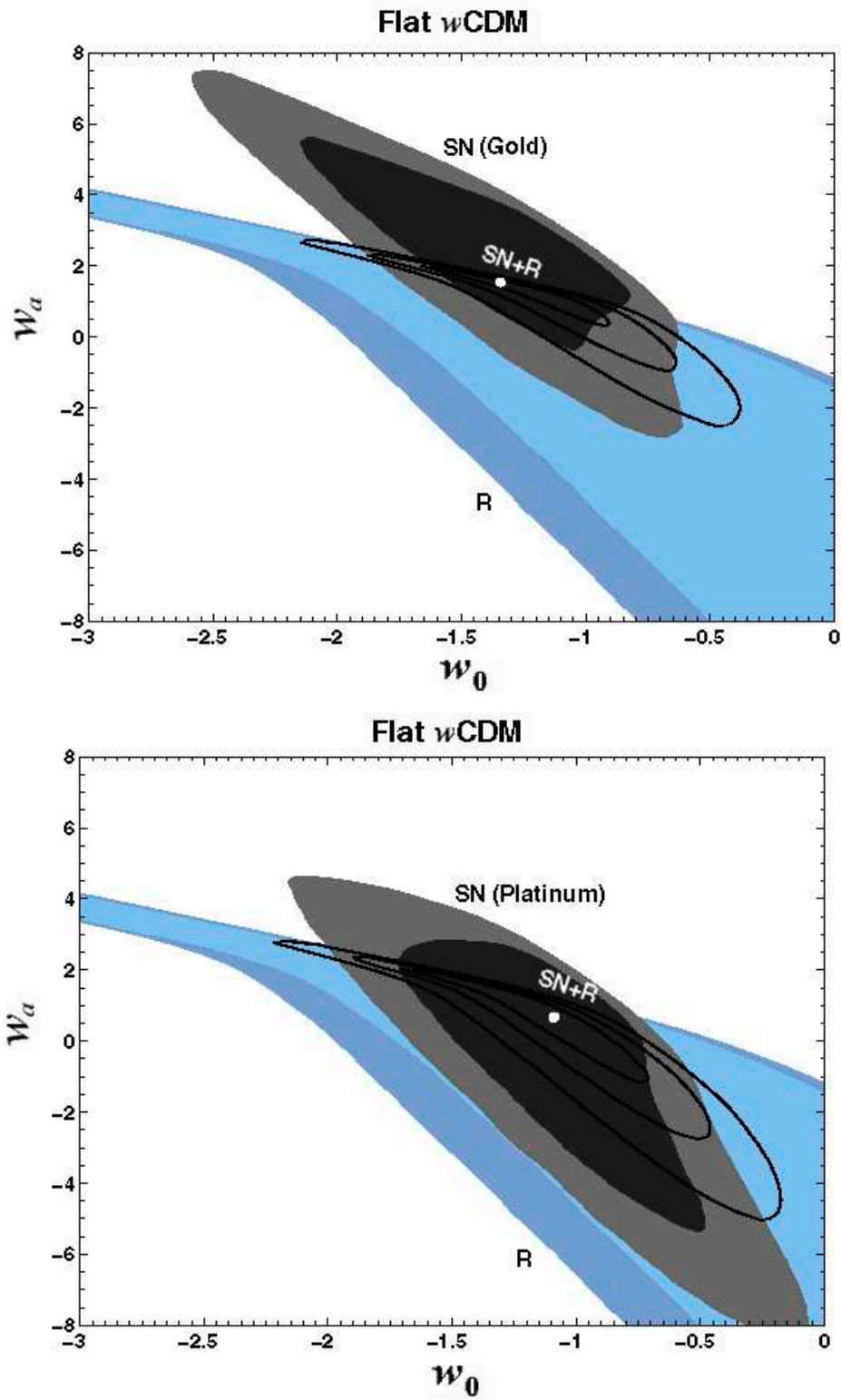


Figure 4: Similar to Fig. 3, but with an equation of state $w(a) = w_0 + w_a(1 - a)$ for $0 \leq z \leq 1089$.

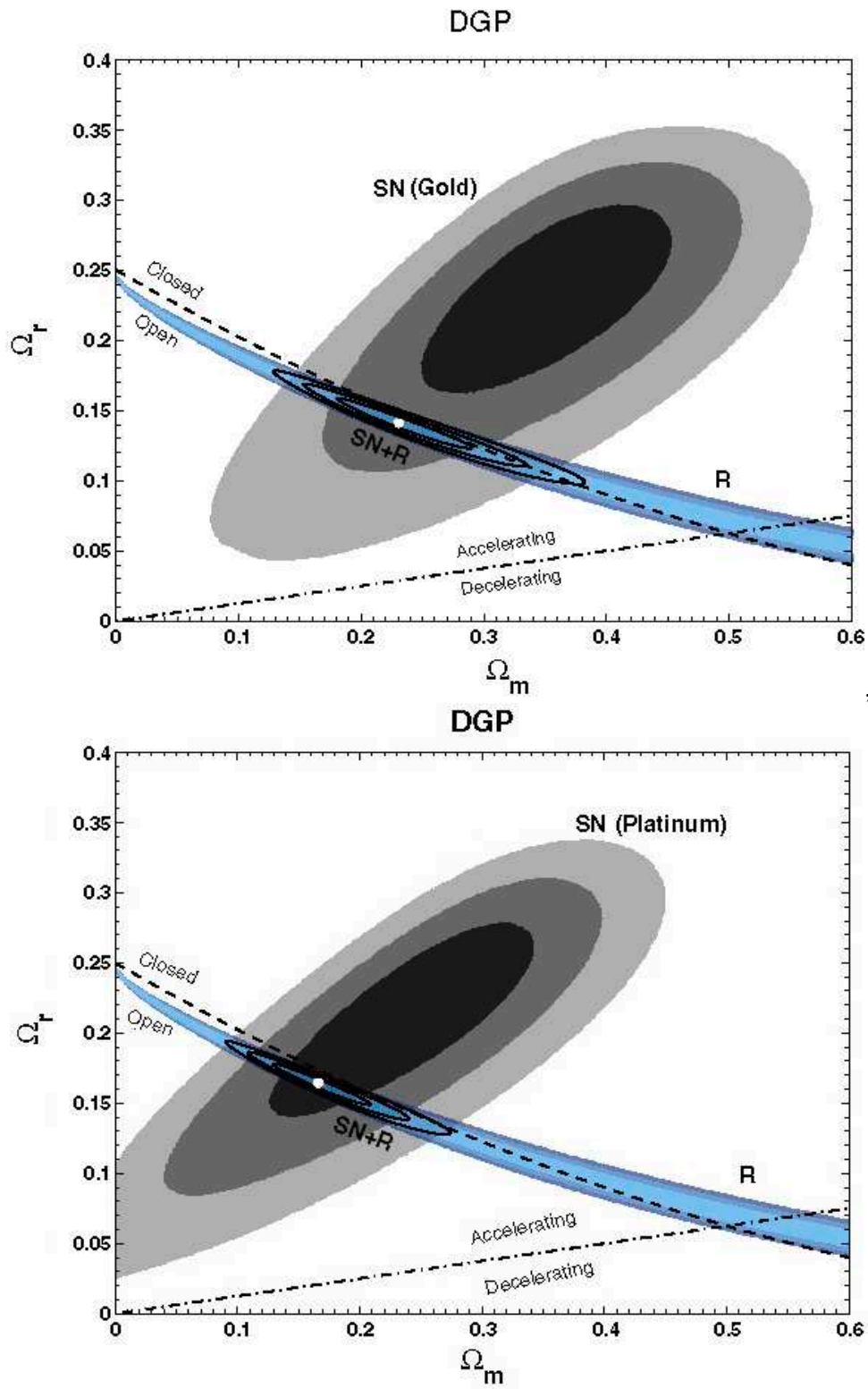


Figure 5: Similar to Fig. 1, but for the DGP model.

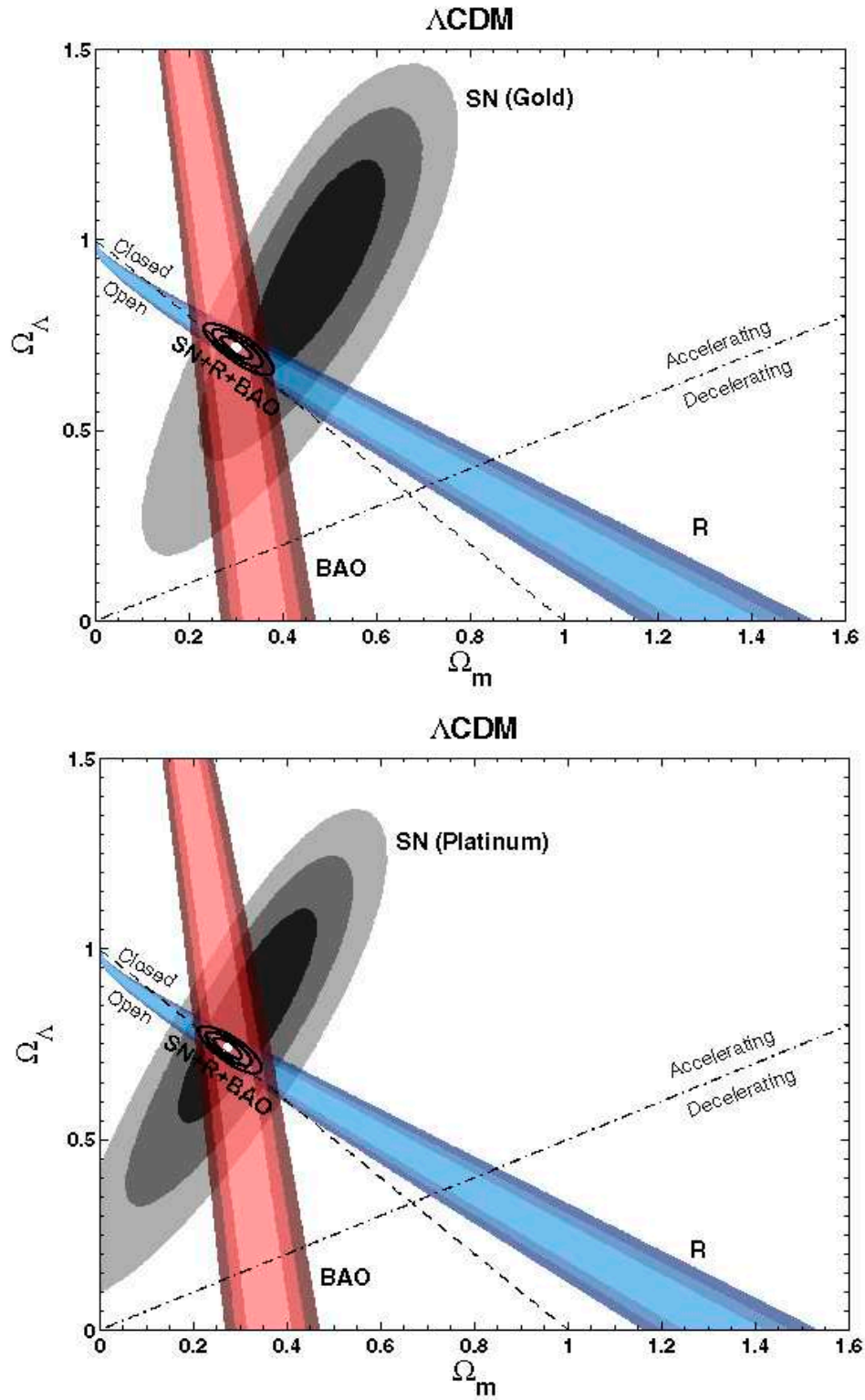


Figure 6: Similar to Fig. 1, but also showing the effect of the BAO constraint on the parameter space.

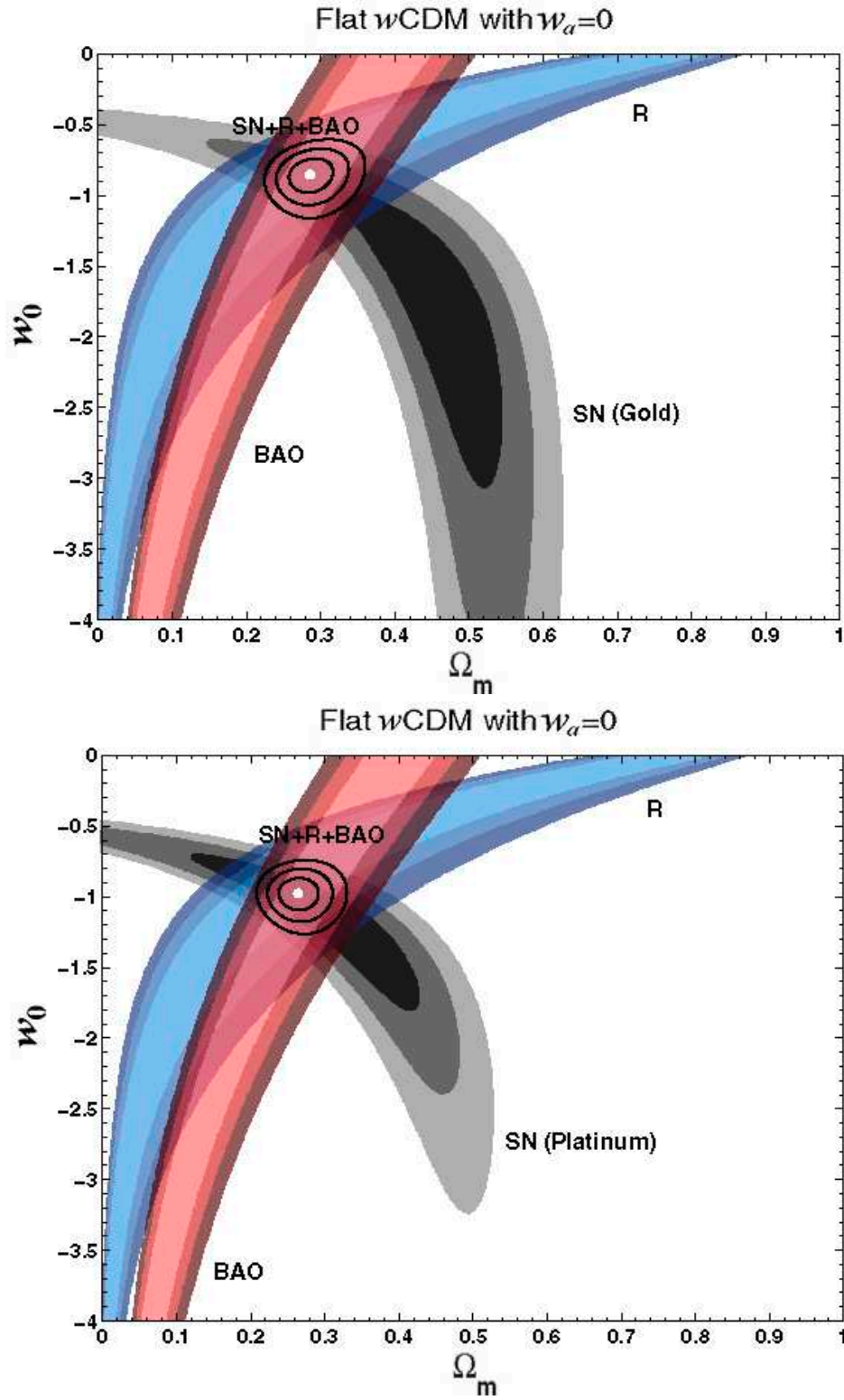


Figure 7: Similar to Fig. 2, but also showing the effect of the BAO constraint on the parameter space.